The Heart Surgery Forum 2022-5067
26 (2), 2023 [Epub March 2023]
doi: 10.1532/hsf.5067

Online address: http://journal.hsforum.com

Adult Bone Marrow-Derived Mesenchymal Stem Cells Seeded on Tissue-Engineered Cardiac Patch Contribute to Myocardial Scar Remodeling and Enhance Revascularization in a Rabbit Model of Chronic Myocardial Infarction

Jue Zhang,[1] Mingjiang Wu,[1] Xiaoqiang Zhang,[2] Mingli Yang,[3] Tingwang Xiong,[1] Wei Zhi[4]

[1]Department of Pharmacy of Zunyi Medical and Pharmaceutical College, Zunyi, Guizhou, P. R. China;
[2]Department of Cardiovascular, Chengdu Second People's Hospital, Chengdu, Sichuan, P. R. China;
[3]Department of Medical Genetics, Zunyi Medical University, Zunyi, Guizhou, P. R. China;
[4]Key Laboratory of Advanced Technologies of Materials (Ministry of Education), School of Materials Science and Engineering, Southwest Jiaotong University, Chengdu, Sichuan, P. R. China

ABSTRACT

Background: Although the transplantation of tissue-engineered cardiac patches with adult bone marrow-derived mesenchymal stem cells (MSCs) can enhance cardiac function after acute or chronic myocardial infarction (MI), the recovery mechanism remains controversial. This experiment aimed to investigate the outcome measurements of MSCs within a tissue-engineered cardiac patch in a rabbit chronic MI model.

Methods: This experiment was divided into four groups: left anterior descending artery (LAD) sham-operation group (N = 7), sham-transplantation (control, N = 7), non-seeded patch group (N = 7), and MSCs-seeded patch group (N = 6). PKH26 and 5-Bromo-2'-deoxyuridine (BrdU) labeled MSCs-seeded or non-seeded patches were transplanted onto chronically infarct rabbit hearts. Cardiac function was evaluated by cardiac hemodynamics. H&E staining was performed to count the number of vessels in the infarcted area. Masson staining was used to observe cardiac fiber formation and to measure scar thickness.

Results: Four weeks after transplantation, a remarkable improvement in cardiac functionality could be distinctly observed, which was most significant in the MSCs-seeded patch group. Moreover, labeled cells were detected in the myocardial scar, with most of them differentiated into myofibroblasts, some into smooth muscle cells, and only a few into cardiomyocytes in the MSCs-seeded patch group. We also observed significant revascularization in the infarct area implanted in either MSCs-seeded or non-seeded patches. In addition, there were significantly greater numbers of microvessels in the MSCs-seeded patch group than in the non-seeded patch group.

Conclusions: MSCs seeded on tissue-engineering cardiac patches contributed to myocardial scar positive remodeling and enhanced neovascularization in a rabbit model of chronic MI. These results indicate that myocardial scar positive remodeling and neovascularization induced by MSCs seeded patch might play critical roles in cardiac function improvement in the tissue engineering treatment of chronic MI.

Received August 8, 2022; accepted November 23, 2022.

Correspondence: Wei Zhi, Key Laboratory of Advanced Technologies of Materials (Ministry of Education), School of Materials Science and Engineering, Southwest Jiaotong University, Chengdu 610031, Sichuan, P. R. China (e-mail: zhiwei7704@163.com).

INTRODUCTION

Recent studies have shown the therapeutic potential of adult bone marrow-derived mesenchymal stem cells (MSCs) for regenerative therapy in various domains [Pittenger 1999; Prockop 1997; Ng 2008; Jones 2008]. Multipotent stem cells derived from bone marrow could be differentiated into cell lineages distinct from the organ in which they reside [Raff 2003] and delivered either in autologous procedures or using an allogeneic strategy. Some reports hypothesized they might be relatively immune-privileged [Le Blanc 2003]. In addition, these cells have proangiogenic properties that are relatively easy to harvest and harbor an excellent expansion capability [Pittenger 1999]. In some related studies and clinical trials, the results of the myocardial cellular therapeutic strategy platform results hypothesize that MSCs could effectively regenerate integrated cardiomyocytes function, inducing neovascularized, reducing infarct size, improving regional and global cardiac contractile function, and protecting against left ventricle adverse remodeling in treatment of myocardial infarction (MI) [Shake 2002; Toma 2002; Chacko 2009; Davani 2003; Chen 2004; Mangi 2003; Hattan 2005; Alfaro 2008]. For the mentioned reasons, the utilization of MSCs emerges as an optimal preference for MI treatment [Wagers 2004]. Despite the encouraging results in many types of correlated research, cellular therapy has some limits. The main limitation is the efficacy of cell engraftment, which is remarkably low as more than 90% of the suspension injected is lost and does not engraft. Therefore, much effort has recently conveyed regarding tissue-engineering advancement strategies to rehabilitate the injured myocardium. Over the past years, several studies in independent laboratories have

demonstrated that the transplantation of tissue-engineered cardiac patches with MSCs can play a vital role in cardiac function rehabilitation after MI. Nevertheless, the outcome of MSCs seeded on patches has been presented and discussed in several results [Potapova 2008; Derval 2008; Chang 2007; Chen 2008; Krupnick 2002]. Whether MSCs can differentiate into cardiac cell lineages and whether the improved heart function is due to the differentiation of MSCs to myocytes or other effects are still unclear.

Our previous experiments showed that an MSCs-seeded patch could improve cardiac function in a chronic MI model, and some indications of differentiation to myocardial cell lineages could be examined [Tan 2009; Liao 2006]. Hence, the present study aimed to determine the outcome measurements of MSC seeded on a tissue-engineered cardiac patch after transplantation in a rabbit model of chronic MI.

METHODS

Cell isolation, culture, and labeling: Allogeneic rabbit MSCs isolation was performed at Osiris Therapeutics, Inc. (Baltimore, Maryland), as previously described [Pittenger 1999]. Briefly, bone marrow aspirates were passed through a density gradient to eliminate unwanted cell types. Hematopoietic cells, fibroblasts, and other non-adherent cells were neutralized during medium changes. The remaining purified MSCs population was further expanded in the culture. The cells were subsequently extracted and labeled with fluorescent dyes with the use of a PKH26 red fluorescent cell linker kit (Sigma), as previously described [Messina 1992], and a 5-Bromo-2-deoxyuridine (BrdU) kit (Roche, Minneapolis, Minnesota). The viability of the labeled cells was confirmed to be larger than 90%, and the fluorescent intensity was 100 times brighter than background autofluorescence. Eventually, the cells were counted and used for seeding on the small intestinal submucosa (SIS) scaffold.

3D culture on SIS scaffolds: The labeled MSCs were seeded at a concentration of 1×106 cells per scaffold on SIS scaffolds (1.5-cm length × 1.5-cm width, thickness: 0.3-0.4 mm) placed in a 6-well plate. The scaffolds were prepared from porcine SIS using a previously described standard procedure [Badylak 1989]. Briefly, a segment of fresh porcine jejunum was extracted and washed in water to remove the tunica mucosa, the serosa, and tunica muscularis of the segment. The obtained SIS was thoroughly rinsed in a saline solution to remove the resident cells and sterilized in 0.1% peracetic acid. Lastly, the SIS sheets were lyophilized and sterilized with ethylene oxide. We seeded the labeled cells on the rehydrated SIS by dropping the cell suspension uniformed on top of the scaffold. The patches were incubated in a humidified atmosphere of 5% CO2 and 95% air at 37 °C for 5-7 days before implantation, with daily medium changes. Non-seeded SIS was prepared following the same method.

The cell construction was observed under a fluorescent inverted phase-contrast microscope for five days before implantation. After culturing the patches with MSCs, they were fixed in 10% phosphate-buffered formalin solution and 2.5% glutaraldehyde, respectively, to examine the quality of patches by light and scan electron microscopes.

Animals: A total of 30 healthy adult male New Zealand white rabbits weighing 1.8-2.1 kg each were subjected to open-chest surgery. This study was reviewed and approved by the Institutional Animal Care and Use Committee of Sichuan University and performed following the Principles of Laboratory Animal Care formulated by the National Society for Medical Research and the Guide for the Care and Use of Laboratory Animals published by the National Institutes of Health of the United States (NIH, publication No. 85-23, revised 1996).

Rabbit model of chronic MI: Our method for the induction of chronic MI was performed, as previously described [Fujita 2004] with minor modifications. Briefly, 24 rabbits were anesthetized with a compound of ketamine (35 mg/kg) and xylazine (5 mg/kg) and maintained with 1% lidocaine injected into subcutaneous. The chest was opened by a median sternotomy using sterile techniques. Chronic MI was produced by permanent ligation of the left anterior descending artery (LAD) at the midpoint between the starting point and the cardiac apex with an intramural stitch. The correct ligation position was confirmed by ST-segment elevation on the ECG and regional pallor of the myocardial surface. Six rabbits were subjected to only an open chest without ligation.

Cardiac patches implantation: Echocardiography was performed to assess left ventricle ejection fraction (LVEF) before cardiac patch implantation (four weeks after LAD coronary artery ligation). Rabbits with LVEF of less than 35% were anesthetized with sodium pentobarbital (30-40 μg/kg, IV), intubated, respiration using mechanical ventilatory support, and under sterile technique, the chest was opened. The infarcted area was visually identified based on the surface scar and wall motion abnormality.

Twenty-one rabbits were randomized to implantation of an MSCs-seeded patch ($N = 7$), non-seeded patch ($N = 7$), or sham-transplantation (control, $N = 7$) onto the infarcted myocardium. The MSCs-seeded or non-seeded patch was attached to the epicardial surface of the ischemic and peri-ischemic myocardium by four sutures. The control group consisted of rabbits subjected to sham transplantation by inserting four sutures into the scar. Additionally, the LAD sham-operation group (sham, $N = 6$) was subjected to an open chest, and four sutures were made. The surgical incision was then sutured in layers. Negative pressure drainage was performed. In an initial series of pilot experiments, the technical aspects of the procedure were refined. After the operation, the rabbits were allowed to recover and given 0.03 mg/kg buprenorphine IM BID and 15mg/kg penicillin IM QD for three days. The rabbits did not receive any immunosuppression therapy.

Functional assessment by cardiac hemodynamic studies: The cardiac hemodynamic evaluation was performed four weeks after cardiac patch graft transplantation, as previously described [Nagaya 2005]. The right carotid artery carefully was isolated, and a carotid arterial catheter was inserted into it and advanced into the left ventricle (LV) to measure LV pressure. A polygraph for the measurements was obtained by

Table 1. Left ventricle hemodynamic parameters between the groups

Variables	Sham operation group (*N* = 6)	Control group (*N* = 5)	MSCs-seeded patches group (*N* = 6)	Non-seeded patches group (*N* = 7)
HR (t/m)	344±38	303±21	322±17	293±50
LVEDP (mmHg)	2.92±1.23	16.21±1.08**	8.73±2.04##	10.99±2.22##
LVSP (mmHg)	114.30±13.72	59.80±3.04**	106.32±11.95##	90.23±17.92##
+dp/dt(mmHg/s)	4418.20±340.93	1297.72±358.75**	4104.63±242.38##&	2778.52±333.54##
-dp/dt(mmHg/s)	-3730.75±276.15	-1046.86±94.35**	-3131.74±331.93##&	-2525.83±217.41##

MSCs, mesenchymal stem cells; SIS, small intestinal submucosa; HR, heart rate; LVEDP, left ventricular end-diastolic pressure; LVSP, left ventricular systolic pressure; +dp/dt, maximum rate of rising in left ventricular pressure during systole; -dp/dt, maximum rate of decrease in left ventricular pressure during diastole. **$P < 0.01$ vs. sham group; #$P < 0.05$ and ##$P < 0.01$ vs. control group; &$P < 0.05$ vs. non-seeded SIS group

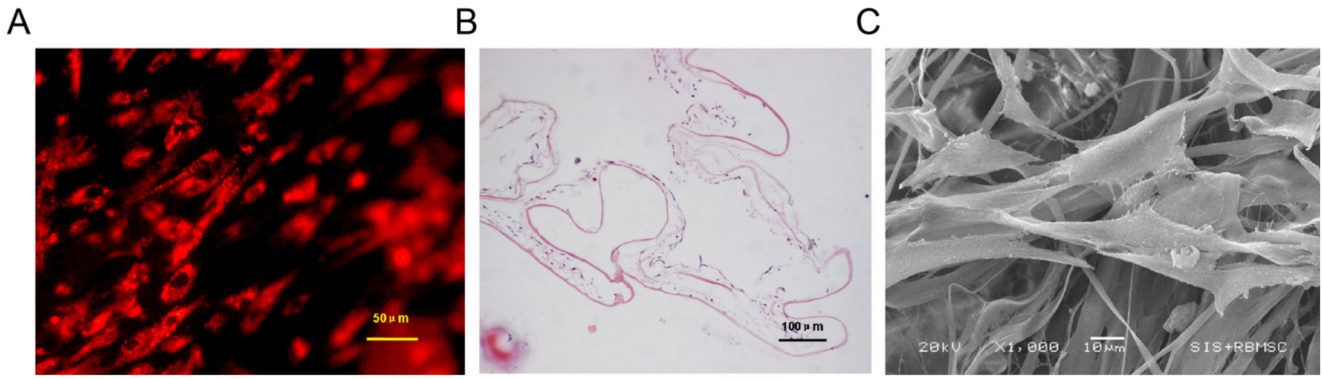

Figure 1. Characteristics of MSC cells on small intestinal submucosa (SIS) scaffold. A) PKH-26 labeled MSCs distributed uniformly on the SIS at co-cultured five days (magnification × 200; scale bar = 50 μm); B) Hematoxylin-eosin staining showed MSCs adhered closely and grew well in a multilayer on SIS (magnification × 100; scale bar = 100 μm); C) SEM showed the cells distributed throughout the scaffold volume, spindle-shaped cells attached to the scaffold and extend pseudopodal. Some extracellular matrices were found around the cells (magnification × 1000; scale bar = 10 μm).

using a pressure transducer. All variables were obtained and averaged on three consecutive cardiac cycles.

Histopathological analysis: Following hemodynamic measurements, the heart of the rabbits was exposed by median sternotomy and obtained in diastole via directly injecting 2-3 mL of 2M KCl into the left ventricle [Piao 2005]. Subsequently, the heart was quickly removed and sliced into four transverse sections from apex to base. Each section's thickness was sliced in half; one was embedded in OCT compound (Miles Scientific), snap-frozen in liquid nitrogen, while the other was fixed in 4% paraformaldehyde and embedded in paraffin. Serial sections of 6-μm thickness were cut, and parts were stained with hematoxylin-eosin (HE) or Masson's Trichrome staining.

Measurement of vascular density: The effect of cardiac patch implantation on angiogenesis was evaluated in paraffin-embedded slices by counting the number of vessels in the infarcted area (10 slices per heart) stained with HE under a light microscope (magnification ×400). Five fields per slice in the infarcted area were selected randomly, and vessels were counted in each field. The number of vessels in each slice was averaged, and the number of vessels per unit area (0.2 mm2) represented vascular density [Tomita 1999].

Fibrogenesis observation and scar thickness measurement: Masson's Trichrome staining was used to observe fibrogenesis and measure scar thickness. To evaluate scar thickness, five transverse sections per heart were randomly extracted from the infarcted region wall, and five randomly selected scar fields per section under light microscopy (magnification ×40) were scanned and computerized by a digital image analyzer to measure scar thickness.

Histological examination: PKH26 identified the survival of engrafted cells seeded on cardiac patches, DAPI-positive cells in frozen sections, and BrdU-positive cells in paraffin sections made from the hearts.

Cardiac-like cells from MSCs were verified by antibody immunostaining for cardiac troponin T (cTnT, Abcam, UK), myosin heavy chain (MHC, Abcam, UK), sarcomeric muscle actin (SMA, Abcam, UK). Briefly, frozen tissue sections were fixed in acetone at 4°C for 10 minutes and incubated separately with a mouse monoclonal immunoglobulin G anti-troponin T or myosin heavy chain or sarcomeric muscle actin for 60 minutes at room temperature. After washing with TBS solution, the sections were incubated with a goat anti-mouse conjugated fluorescein immunoglobulin G for primary antibodies. According to the manufacturer's recommendations,

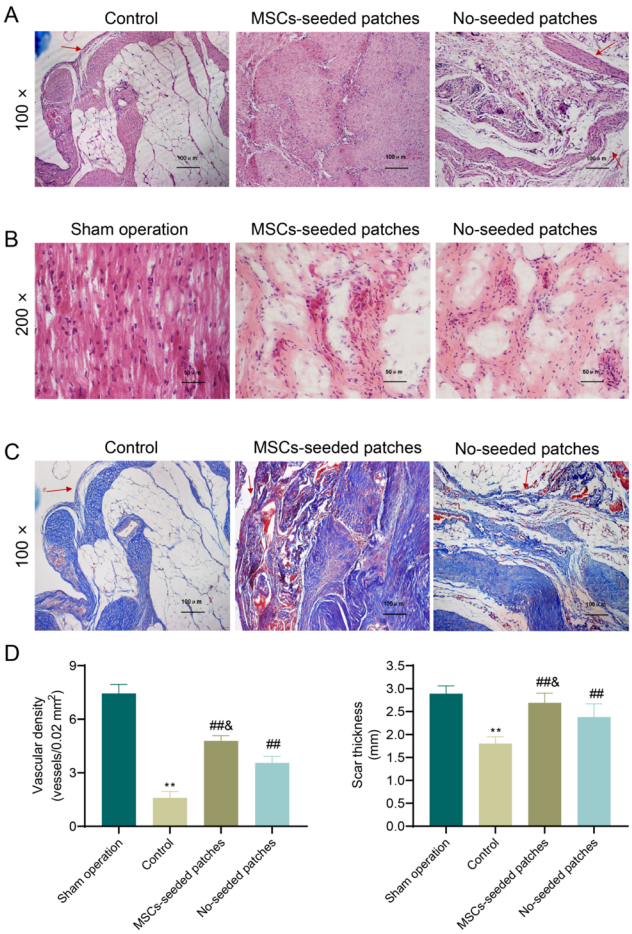

Figure 2. Histological staining of the infarcted area four weeks after implantation. A-B) H&E staining of the infarcted area and neovascularization within the infarcted myocardium scar in the MSCs-seeded patches and non-seeded patches groups, the interstitial cells were significantly increased in the MSCs-seeded patches and non-seeded patches groups; C) Masson trichrome staining of cardiac tissue, arrows represent epicardial layer. New collagen can be seen to have deposited within the scar in the MSCs-seeded patches and non-seeded patches groups; D) Left ventricle vascular density in the scar tissue and scar thickness in the infarcted region. The vascular density in the MSCs-seeded patches group is higher than in the non-seeded patches group or the control group. The scar thickness in the two treatment groups is higher than in the control group. $^{**}P < 0.01$ vs. sham operation group; $^{\#\#}P < 0.01$ vs. control group; $P < 0.05$ vs. MSCs-seeded patches group.

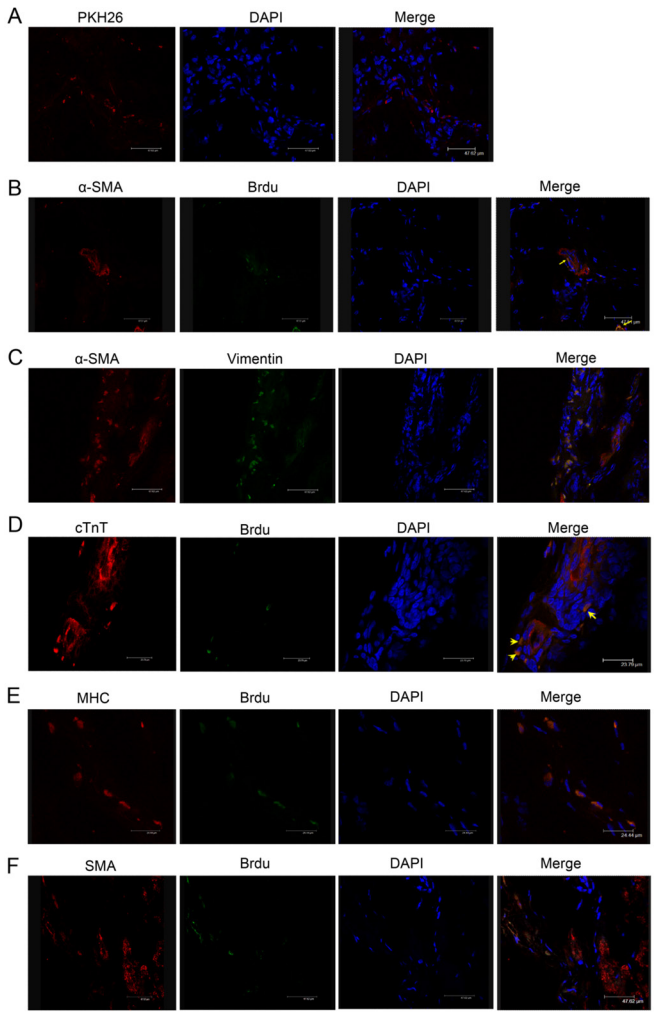

Figure 3. Stem cell migration and differentiation in the infarcted area four weeks after implantation. A) PKH26 -positive MSCs were detected in the infarct areas; B) BrdU-positive MSCs (green) participated in vessel formation (red); C) MSCs differentiated to myofibroblasts expressed αSMA (red) and Vimentin (green) within the scar tissue; D-F) Only very few cells were double positive for the BrdU (green) and the cardiac markers (red): cardiac troponin T (cTnT, D) or myosin heavy chain (MHC, E) or sarcomeric muscle actin (F). Nuclear staining by DAPI (blue).

the neovascular transformation of MSCs was verified by antibody immunostaining for α-smooth muscle actin (α-SMA, Abcam, UK). Myofibroblast transformation of MSCs was confirmed by antibody immunostaining for Vimentin (Sigma, USA) and α-SMA (Abcam, UK).

Statistical analysis: Numerical values are presented as mean ± standard error of mean (SEM). All analyses were performed using the SPSS software for Windows (version 15.0). Comparisons of parameters between the two groups were made with an unpaired Student t-test. Comparisons of parameters among three groups were made with a one-way ANOVA, followed by the Scheffe multiple-comparison test. Comparisons of changes in parameters among the three groups were made by a two-way ANOVA for repeated measures, followed by the Scheffe multiple-comparison test. A P-value < 0.05 was considered significant.

RESULTS

General condition of rabbits: Overall, 30 rabbits were included in the present study. Two rabbits died within four weeks after LAD ligation, and one rabbit was excluded because its LVEF was above 35%. The MSCs-seeded patches group

included seven rabbits, of which one died after implantation. The non-seeded patches group included seven rabbits, of which none died after implantation. The untreated control group included seven rabbits, of which two died after MI during the follow-up period, due to severe heart failure. Additionally, a LAD sham-operation group included six rabbits. Thus, the final hemodynamic study analysis was performed on 24 rabbits.

Characteristics of cell constructs: The SIS scaffold in the present study is a nonimmunogenic, biodegradable, biocompatible collagen matrix and possesses tissue-specific regeneration properties [Badylak 1989]. The scaffolds were smoothly saturated with the aqueous medium, and the hydrated matrix appeared transparent and displayed a soft consistency. Under a fluorescent microscope, PKH-26 labeled MSCs were observed to distribute uniformly on the SIS (Figure 1A). (Figure 1) H&E staining showed MSCs adhered closely and grew well in a multilayer on SIS (Figure 1B). Scan electron microscope (SEM) showed the cells uniformly distributed throughout the scaffold volume, spindle-shaped cells tightly attached to the surface of the porous and 3-dimensional scaffolds, and extended pseudopodal. Some extracellular matrices could be seen around the cells (Figure 1C).

Assessment of cardiac function measures by hemodynamic studies: Four weeks after implantation, LV end-diastolic pressure (LVEDP) illustrated a marked elevation in the control group, which was significantly reduced in the MSCs-seeded patches group and non-seeded patches group. LV systole pressure (LVSP) demonstrated a decrease in the control group, which was dramatically increased in both of the treatment groups. LV maximum dP/dt was significantly higher in the sham-operation group than in the control group. Still, LV absolute maximum dP/dt was improved considerably in either of the treatment groups, and the MSCs-seeded patches group was significantly more effective than the non-seeded patches group. There was no significant difference in heart rate among the four groups. The data of hemodynamic studies indicated LV dysfunction and dilation in the control group by the increased LVEDP and the decreased LVSP. Also, LV function improvement in the treatment groups could be seen by the decreased LVEDP and the increased LVSP and LV absolute maximum dP/dt. (Table 1)

Histopathological evaluation: H&E staining showed neovascularization within infarcted myocardium scar in either of the treatment groups. The implanted patches four weeks after implantation were wholly integrated with the host connective tissue and partially dissolved. Around the patches, infiltration of lymphocytes and macrophages was observed. The number of interstitial cells was significantly increased in both treatment groups (Figure 2A). (Figure 2) Small myocyte-like cells grew between collagen bundles in the MSCs-seeded group in some frozen sections. Some displayed normal parallel arrangements of myocytes, whereas others were randomly oriented (Figure 2B).

Masson's trichrome staining demonstrated new collagen deposition within the scar, leading to significant fibrogenesis in either treatment groups. The collagen density was significantly higher in the MSCs-seeded group than in the non-seeded group (Figure 2C).

Vascular density was notably higher in the ischemic myocardium of the treatment groups than in the control group. However, the vascular density in the MSCs-seeded group was significantly higher than in the non-seeded group (Figure 2D). The wall thickness of LV for both treatment groups, specifically the MSCs-seeded group, was more occupied than that of the control group. However, the LV wall thickness of the two treatment groups did not recover to the level observed in the sham-operation group (Figure 2D).

Stem cell migration and differentiation in ischemic myocardium: Four weeks after MSCs-seeded SIS transplantation, immunofluorescence showed that PKH26-labeled MSC cells migrated into the post-infarction ventricular wall and localized primarily in the scar tissue from the patches implanted on the epicardial surface of MI (Figure 3A). (Figure 3) In addition, the BrdU-positive MSCs participated in vessel formation, and others formed vascular structures in the ischemia myocardium (Figure 3B). The large BrdU-positive MSCs differentiated to myofibroblasts expressed α-SMA and Vimentin within the scar tissue (Figure 3C). Only very few cells were double positive for the BrdU and the cardiac-specific markers (Figures 3D-3F).

DISCUSSION AND CONCLUSION

The current study showed that MSCs seeded in an SIS patch implanted on the epicardial surface of an infarct myocardium could migrate and survive into the scar tissue, contribute to positive scar remodeling, and enhance neovascularization in a rabbit model of chronic MI.

Recent studies have illustrated that implantation of MSCs-seeded tissue-engineered cardiac patches improved cardiac function in the experimental models of MI [Potapova 2008; Derval 2008; Chang 2007; Chen 2008; Krupnick 2002]. Several possible mechanisms explained the improvement of postinfarct remodeling and cardiac function by implanting the tissue-engineered cardiac patch. However, the therapeutic effects of MSCs as seed cells remain controversial. Krupnick et al. first seeded MSCs on a 3D matrix and demonstrated that MSCs on the scaffold differentiated into cardiac cell linage within the left ventricle in a rat model. Potapova et al. and Chang et al. had similar conclusions in a canine and rat model. However, Derval et al. reported that MSCs seeded on muscle patches increase the scar's repopulation and thickness without cardiac lineage differentiation. Differences in the phase of MI, the various biomaterials for patch and animal models, and the implantation technologies might explain the reported discrepancies. Our previous studies [Tan 2009; Liao 2006] showed that SIS not only provided mechanical and physical support to the damaged cardiac tissue after MI but also acted as a support for the delivered MSCs implants in a rabbit model of chronic MI. Thus, we employed this model to observe the role MSCs seeded on SIS play in improving myocardium infarction.

In this present study, PKH26 and BrdU double-labeled MSCs were traced in the infarct and periinfarct areas of the heart. We found numerous labeled cells in the scar. In

contrast, only a few colocalized with cardiac muscle-specific proteins, indicating a lack of specific cell signaling in chronic MI settings, in which the tissue injury cascade and compensatory response are different from acute cMI. MSCs myogenesis may require rapid and massive activation of the inflammatory cascade, which is present in acute MI and responsible for inflammatory cell infiltration.

In our study, many labeled MSCs distributed in scar tissue were positive for myofibroblast markers with α-smooth muscle actin (α-SMA) and Vimentin, suggesting MSCs differentiated into myofibroblasts. An early study indicated that MI tissues transform into scar tissues at the chronic stage through granulation tissue consisting of numerous myofibroblasts that underwent apoptosis and were gradually lost after one week. The apoptosis damaged scar tissue and enhanced heart adverse remodeling [Takemura 1998]. Myofibroblasts are progenitor cells of fibroblasts that generate collagen fibers and are central to fibrogenesis at remodeling sites after myocardial injury [Sun 1996; Weber 1995]. A recent study [Frangogiannis 2002] suggested that myofibroblasts are not only collagen-producing cells in MI but may instead serve as a versatile cell population assuming different phenotypes, such as precursor cells necessary for angiogenesis, depending on the physiological needs.

Interestingly, in Masson's trichrome staining sections, we found more intensive collagen deposition in a scar in MSCs-seeded than in the non-seeded patch group and control group, and quantitative morphometry revealed the scar thickness increased in the MSCs-seeded patch group compared with the non-seeded patch group or control group, suggesting reduced scar adverse remodeling in MSCs-seeded patch group. These indicate that MSCs may be induced to differentiate into myofibroblasts under chronic ischemia and tissue hypoxia and prevent adverse remodeling by changing the geometry and structural characteristics of the scar. The determination of MSCs lineage-specific differentiation may better understand the infarcted myocardium regional microenvironment produced by various models. Thus, our finding provides new evidence in the literature that MSCs migrated from their seeded patch into scar tissue might contribute to fibrogenesis in the setting of chronic MI.

In our study, some of the labeled MSCs present on vessel walls within scars were positive for α-SMA and negative for Vimentin, suggesting their differentiation into smooth muscle cells and participation in vessel formation. This differentiation has enhanced the significant increase of vessel density in the ischemia and scar areas of the MSCs-seeded patch group. MSCs can induce angiogenesis by providing angiogenic factors such as vascular endothelial growth factor (VEGF) and essential fibroblast growth factor (bFGF) [Kamihata 2001; Kinnaird 2004]. Kinnaird et al. [Kinnaird 2004] demonstrated that MSCs produced various arteriogenic cytokines, and these effects appeared to be mediated through the paracrine pathway associated with the local release of these cytokines. Therefore, MSCs may have participated in or triggered an angiogenic process. More specifically, our previous study reported that SIS as an acellular extracellular matrix scaffold could provide cytokines, including VEGF, to induce neovascularization. These suggest that long-term tissue hypoxia and interaction between MSCs and SIS may drive MSCs to enhance neovascularization in chronic ischemia myocardium.

We also evaluated the functional improvement seen after patch implantation by hemodynamic study. Four weeks after LAD ligation, a progressive decline in LV function values at rest was observed. MSCs and SIS contributed to preserving resting LV function four weeks after cardiac patch implantations (eight weeks after LAD ligation), thus restoring it to near the sham-operation group values in the treatment groups. In contrast, the control group showed a progressive decline in LV function. Angiogenesis and scar positive remodeling may contribute to the maintenance of cardiac function by preserving residual, viable cardiomyocytes [Miyagawa 2002; Mollmann 2006], and neovascularization might also restore contractility in hibernating areas of the myocardium [Kocher 2001]. Accordingly, the significant increase in collagen deposition and vessel density and the differentiation into myofibroblasts and smooth muscle cells seen in the MSCs-seeded patch group might have contributed to the preservation of LV function at rest, thus indicating that MSCs seeded on SIS might have therapeutic effects independent on SIS.

The survival and homing of engrafted cells into the ischemia tissue are thought to play a crucial role in the success of tissue engineering therapy. In this present study, MSCs were seeded on SIS to construct a tissue-engineered cardiac patch and delivered on the epicardial surface of the infarct myocardium. PKH26- and BrdU-positive MSCs were distributed to the whole scar area in this model. However, it was thought that homing signals might be more intense in acute ischemic syndromes than in chronic ischemia properties. This might account for the homing signal of MSCs to mobilize and migrate into the ischemia tissue intended through the micro-environment constructed by tissue-engineered cardiac patch graft.

All these discussed results above might have even greater significance because of the allogeneic nature of MSCs and the fact that treated rabbits in our study received no immunosuppression therapy. MSCs from humans and other species have a cell surface phenotype that is poorly immunogenic. Recent studies, including our previous experiments, showed that long-term allogeneic MSCs could construct tissue-engineered tissue engrafts in various tissues without immunosuppression. These data suggest that allogeneic MSCs may have the apparent advantage of clinical availability over autologous stem cells in different clinical settings.

The present study had some limitations. First, the number of animals in each group was relatively small, which might have limited conclusions about efficacy to a certain extent. Second, the follow-up in the present study was only up to four weeks after implantation. A longer follow up might be needed to confirm that the scar-positive remodeling and heat functional amelioration are preserved for a more extended period after the degradation of the SIS from the epicardial surface of the ischemic area. Lastly, immunohistochemical evidence cannot support the differentiation of MSCs into vascular endothelial cells due to a lack of anti-rabbits vascular

endothelial cell primary antibodies. In addition, for a similar reason, an assessment of MSCs proliferation and development in vivo was not performed, which may have created a certain level of bias.

In conclusion, our experiments provide a novel proof of concept for MSCs used in a tissue-engineering treatment strategy of implantation into chronically ischemic myocardium that is safe and effective. MSCs migrated into scar tissue and differentiated into smooth muscle cells and myofibroblasts, resulting in positive scar remodeling and enhanced neovascularization. Thus, MSCs constructed tissue-engineered cardiac patch implantation has excellent potential as a new therapeutic strategy for treating chronic myocardium infarction.

ACKNOWLEDGEMENT

Funding sources: This research was supported by The project of Guizhou high-level innovative talents training (Zunyi science and technology cooperation project[2017]22); The Project of Zunyi Science and Technology Department (Zunyi science and technology cooperation project HZ[2021]214; HZ [2020]36); The Project of Guizhou Province Science and Technology Department (Guizhou science and technology cooperation [2018]5772-043).

REFERENCES

Alfaro MP, Pagni M, Vincent A, et al. 2008. The Wnt modulator sFRP2 enhances mesenchymal stem cell engraftment, granulation tissue formation and myocardial repair. Proc Natl Acad Sci U S A. 105(47):18366-18371.

Badylak SF, Lantz GC, Coffey A, Geddes LA. 1989. Small intestinal submucosa as a large diameter vascular graft in the dog. J Surg Res. 47(1):74-80.

Chacko SM, Khan M, Kuppusamy ML, et al. 2009. Myocardial oxygenation and functional recovery in infarct rat hearts transplanted with mesenchymal stem cells. Am J Physiol Heart Circ Physiol. 296(5):H1263-1273.

Chang Y, Lai PH, Wei HJ, et al. 2007. Tissue regeneration observed in a basic fibroblast growth factor-loaded porous acellular bovine pericardium populated with mesenchymal stem cells. J Thorac Cardiovasc Surg. 134(1):65-73, 73 e61-64.

Chen CH, Wei HJ, Lin WW, et al. 2008. Porous tissue grafts sandwiched with multilayered mesenchymal stromal cell sheets induce tissue regeneration for cardiac repair. Cardiovasc Res. 80(1):88-95.

Chen SL, Fang WW, Ye F, et al. 2004. Effect on left ventricular function of intracoronary transplantation of autologous bone marrow mesenchymal stem cell in patients with acute myocardial infarction. Am J Cardiol. 94(1):92-95.

Davani S, Marandin A, Mersin N, et al. 2003. Mesenchymal progenitor cells differentiate into an endothelial phenotype, enhance vascular density, and improve heart function in a rat cellular cardiomyoplasty model. Circulation. 108 Suppl 1(II253-258.

Derval N, Barandon L, Dufourcq P, et al. 2008. Epicardial deposition of endothelial progenitor and mesenchymal stem cells in a coated muscle patch after myocardial infarction in a murine model. Eur J Cardiothorac Surg. 34(2):248-254.

Frangogiannis NG, Shimoni S, Chang SM, et al. 2002. Active interstitial remodeling: an important process in the hibernating human myocardium. J Am Coll Cardiol. 39(9):1468-1474.

Fujita M, Morimoto Y, Ishihara M, et al. 2004. A new rabbit model of myocardial infarction without endotracheal intubation. J Surg Res. 116(1):124-128.

Hattan N, Kawaguchi H, Ando K, et al. 2005. Purified cardiomyocytes from bone marrow mesenchymal stem cells produce stable intracardiac grafts in mice. Cardiovasc Res. 65(2):334-344.

Jones E, McGonagle D. 2008. Human bone marrow mesenchymal stem cells in vivo. Rheumatology (Oxford). 47(2):126-131.

Kamihata H, Matsubara H, Nishiue T, et al. 2001. Implantation of bone marrow mononuclear cells into ischemic myocardium enhances collateral perfusion and regional function via side supply of angioblasts, angiogenic ligands, and cytokines. Circulation. 104(9):1046-1052.

Kinnaird T, Stabile E, Burnett MS, et al. 2004. Local delivery of marrow-derived stromal cells augments collateral perfusion through paracrine mechanisms. Circulation. 109(12):1543-1549.

Kinnaird T, Stabile E, Burnett MS, et al. 2004. Marrow-derived stromal cells express genes encoding a broad spectrum of arteriogenic cytokines and promote in vitro and in vivo arteriogenesis through paracrine mechanisms. Circ Res. 94(5):678-685.

Kocher AA, Schuster MD, Szabolcs MJ, et al. 2001. Neovascularization of ischemic myocardium by human bone-marrow-derived angioblasts prevents cardiomyocyte apoptosis, reduces remodeling and improves cardiac function. Nat Med. 7(4):430-436.

Krupnick AS, Kreisel D, Engels FH, et al. 2002. A novel small animal model of left ventricular tissue engineering. J Heart Lung Transplant. 21(2):233-243.

Le Blanc K. 2003. Immunomodulatory effects of fetal and adult mesenchymal stem cells. Cytotherapy. 5(6):485-489.

Liao B, Deng L, & Wang F. 2006. [Effects of bone marrow mesenchymal stem cells enriched by small intestinal submucosal films on cardiac function and compensatory circulation after myocardial infarction in goats]. Zhongguo Xiu Fu Chong Jian Wai Ke Za Zhi. 20(12):1248-1252.

Mangi AA, Noiseux N, Kong D, et al. 2003. Mesenchymal stem cells modified with Akt prevent remodeling and restore performance of infarcted hearts. Nat Med. 9(9):1195-1201.

Messina LM, Podrazik RM, Whitehill TA, et al. 1992. Adhesion and incorporation of lacZ-transduced endothelial cells into the intact capillary wall in the rat. Proc Natl Acad Sci USA. 89(24):12018-12022.

Miyagawa S, Sawa Y, Taketani S, et al. 2002. Myocardial regeneration therapy for heart failure: hepatocyte growth factor enhances the effect of cellular cardiomyoplasty. Circulation. 105(21):2556-2561.

Mollmann H, Nef HM, Kostin S, et al. 2006. Bone marrow-derived cells contribute to infarct remodelling. Cardiovasc Res. 71(4):661-671.

Nagaya N, Kangawa K, Itoh T, et al. 2005. Transplantation of mesenchymal stem cells improves cardiac function in a rat model of dilated cardiomyopathy. Circulation. 112(8):1128-1135.

Ng F, Boucher S, Koh S, et al. 2008. PDGF, TGF-beta, and FGF signaling is important for differentiation and growth of mesenchymal stem cells (MSCs): transcriptional profiling can identify markers and signaling pathways important in differentiation of MSCs into adipogenic,

chondrogenic, and osteogenic lineages. Blood. 112(2):295-307.

Piao H, Youn TJ, Kwon JS, et al. 2005. Effects of bone marrow derived mesenchymal stem cells transplantation in acutely infarcting myocardium. Eur J Heart Fail. 7(5):730-738.

Pittenger MF, Mackay AM, Beck SC, et al. 1999. Multilineage potential of adult human mesenchymal stem cells. Science. 284(5411):143-147.

Potapova IA, Doronin SV, Kelly DJ, et al. 2008. Enhanced recovery of mechanical function in the canine heart by seeding an extracellular matrix patch with mesenchymal stem cells committed to a cardiac lineage. Am J Physiol Heart Circ Physiol. 295(6):H2257-2263.

Prockop DJ. 1997. Marrow stromal cells as stem cells for nonhematopoietic tissues. Science. 276(5309):71-74.

Raff M. 2003. Adult stem cell plasticity: fact or artifact? Annu Rev Cell Dev Biol. 19(1-22).

Shake JG, Gruber PJ, Baumgartner WA, et al. 2002. Mesenchymal stem cell implantation in a swine myocardial infarct model: engraftment and functional effects. Ann Thorac Surg. 73(6):1919-1925; discussion 1926.

Sun Y, Weber KT. 1996. Angiotensin converting enzyme and myofibroblasts during tissue repair in the rat heart. J Mol Cell Cardiol. 28(5):851-858.

Takemura G, Ohno M, Hayakawa Y, et al. 1998. Role of apoptosis in the disappearance of infiltrated and proliferated interstitial cells after myocardial infarction. Circ Res. 82(11):1130-1138.

Tan MY, Zhi W, Wei RQ, et al. 2009. Repair of infarcted myocardium using mesenchymal stem cell seeded small intestinal submucosa in rabbits. Biomaterials. 30(19):3234-3240.

Toma C, Pittenger MF, Cahill KS, Byrne BJ, Kessler PD. 2002. Human mesenchymal stem cells differentiate to a cardiomyocyte phenotype in the adult murine heart. Circulation. 105(1):93-98.

Tomita S, Li RK, Weisel RD, et al. 1999. Autologous transplantation of bone marrow cells improves damaged heart function. Circulation. 100(19 Suppl):II247-256.

Wagers AJ, Weissman IL. 2004. Plasticity of adult stem cells. Cell. 116(5):639-648.

Weber KT, Sun Y, Katwa LC, Cleutjens JP. 1995. Connective tissue: a metabolic entity? J Mol Cell Cardiol. 27(1):107-120.